Journal of Hazardous Materials 177 (2010) 362–371

Contents lists available at ScienceDirect

Journal of Hazardous Materials

journal homepage: www.elsevier.com/locate/jhazmat

Sorption kinetics and equilibrium for the removal of nickel ions from aqueous phase on calcined Bofe bentonite clay

M.G.A. Vieira[a], A.F. Almeida Neto[a], M.L. Gimenes[b], M.G.C. da Silva[a,*]

[a] UNICAMP/FEQ/DTF, Campinas/SP, Brazil
[b] UEM/CTC/DEQ, Maringá/PR, Brazil

ARTICLE INFO

Article history:
Received 28 September 2009
Received in revised form 7 December 2009
Accepted 7 December 2009
Available online 16 December 2009

Keywords:
Sorption
Bentonite clay
Nickel
Heavy metal removal

ABSTRACT

In this paper the kinetics and dynamics of nickel adsorption on calcined Bofe bentonite clay were studied. The clay was characterized through EDX, surface area (BET) and XRD analysis. The influence of parameters (pH, amount of adsorbent, adsorbate concentration and temperature) was investigated. Kinetic models were evaluated in order to identify potential adsorption process mechanisms. The Langmuir and Freundlich models were utilized for the analysis of adsorption equilibrium. Thermodynamic parameters were assessed as a function of the process temperature. The kinetics data were better represented by the second-order model. The process was found to be strongly influenced by the factors studied. The Bofe clay removed nickel with maximum adsorption capacity of 1.91 mg metal/g of clay (20 °C; pH 5.3) and that the thermodynamic data indicated that the adsorption reaction is spontaneous and of an exothermal nature. The Langmuir model provided the best fit for sorption isotherms.

1. Introduction

Water contamination by heavy metals in industrial effluents is a serious environmental problem, leading to the development of studies aimed at their reduction or elimination and waste processing by physical, chemical, thermal, biological or mixed means.

Several studies have shown that the selectivity and efficiency in the removal of pollutants such as heavy metals from effluents by an adsorption process are strongly dependent upon the physical properties and chemical composition of adsorbents.

The literature reports countless studies on heavy metal removal from waters and effluents, including chemical precipitation, physical treatment, such as ion exchange, solvent extraction and adsorption. However, due to the high maintenance and import costs of chemicals or conventional adsorbents, some methods have become unsustainable.

Among heavy metals, nickel is one of the most widely used in western society for the manufacture of stainless steel, superalloys, metal alloys, coins, batteries, etc. Direct exposure to nickel causes dermatitis. Some nickel compounds, such as nickel carbonyl, are cancerigenic and easily absorbed by the skin. The exposure to this compound, at an atmospheric concentration of 30 ppm for half an hour, is lethal [1].

Clay application for sorption or elimination of heavy metals present in effluents has been focused in a number of studies due to countless economic advantages [2–4]. The cost of clays is relatively low as compared to other alternative adsorbents, including activated carbon, natural and synthetic zeolites, ion-exchange resins, and other adsorbent materials. Clays and minerals such as montmorillonite, vermiculite, illite, kaolinite and bentonite are among the natural materials that have been investigated as heavy metal adsorbents [5,6]. Another advantage in using clays as adsorbents is their intrinsic properties, such as large specific surface area, excellent physical and chemical stability, and a number of other structural and surface properties [7].

Abollino et al. [8] observed that Na-montmorillonite adsorbs Cd, Cr, Cu, Mn, Ni, Pb or Zn even in the presence of organic substances (ligands). In Covelo et al. [9] Cd, Cr, Cu, Ni, Pb and Zn were adsorbed on mineral clays simultaneously from solutions at different concentrations.

Currently, the smectite clays of bentonite type are among the most investigated clays for heavy metal removal. The smectite clays of Paraíba generally have CEC values between 50 and 90 meq/100 g of clay [10]. The bentonite clay can be calcium, sodium or polycationic type. The bentonite clays have large surface area (up to 800 m^2/g) and form thixotropic gels. Some cations cause such an intense expansion that crystal layers can be broken down to their single cell. The clays that have Na^+ as the predominant cation, are known to swell in the presence of water, increasing several times its original volume, because the Na^+ allows many water molecules

* Corresponding author at: State University of Campinas, School of Chemical Engineering, Department of Thermofluidynamic Cidade Universitária "Zeferino Vaz" - P.O. Box 6066, 13083-970, Campinas – SP, Brazil. Tel.: +55 19 35213928; fax: +55 19 35213922.
E-mail address: meuris@feq.unicamp.br (M.G.C. da Silva).

0304-3894/$ – see front matter © 2009 Elsevier B.V. All rights reserved.
doi:10.1016/j.jhazmat.2009.12.040

Nomenclature

b, q_m	Langmuir coefficients representing the equilibrium constant for the adsorbate–adsorbent equilibrium and the maximum adsorbed amount on the monolayer
C	intraparticle diffusion model constant
C_{eq}	concentration of metal ions in the liquid phases ($mg\,L^{-1}$)
C_i, C_f	initial and final concentration of metal ion in liquid phase, respectively ($mg\,L^{-1}$)
k_1	pseudo-first-order adsorption rate constant
k_2	second-order adsorption rate constant
K_d	adsorbate distribution coefficient (=q_{eq}/C_{eq} em L/g)
K_f and n	Freundlich coefficients
K_i	intraparticle diffusion rate constant
m	mass of adsorbent (g)
Q	adsorbed mass of metal ion per gram of adsorbent ($mg\,g^{-1}$)
q_{eq}	concentration of metal ions in solid phase at equilibrium ($mg\,g^{-1}$)
q_t	adsorbed amount per unit mass at any given time t
R	universal gas constant (8.314×10^{-3} kJ/(K mol))
R_L	curvature of the sorption isotherm
T	temperature (K)
V	volume of solution (L)
ΔG	Gibbs free energy variation (kJ/mol)
ΔH	enthalpy variation (kJ/mol)
ΔS	entropy variation (J/(K mol))

be adsorbed, increasing the distance between the layers and consequently, separating the clay particles from each other. In the case of polycationic or calcium clay, the amount of adsorbed water is limited and the particles remain attached to each other by electrical and mass interactions [11]. These characteristics confer bentonite highly specific properties which have warranted a wide range of applications in several fields [10].

Although the results involving metal removal by clays are significant and promising, these results still need to be better understood regarding the properties of adsorbents for optimizing the conditions of the process.

The aim of this paper was to study the kinetics and dynamics of nickel adsorption on calcined Bofe bentonite clay in finite bath. The Bofe clay *in natura* and calcined (before and after subjected to nickel adsorption) was characterized as to its chemical composition through EDX, besides surface area (BET method) and X-ray diffraction analysis. The influence of several parameters, such as pH, adsorbent amount, adsorbate concentration and temperature were investigated. Kinetic models were tested to identify the potential adsorption process mechanisms. The Langmuir and Freundlich models were utilized for analysis of the adsorption equilibrium. The thermodynamic parameters were assessed as a function of the process temperature.

2. Theoretical fundamentals

Kinetics for clay–metal interaction was studied thoroughly in this work by applying the following equations and models. Lagergren equation (Lagergren, 1898) [12] expressed by Eq. (1) was applied first assuming pseudo-first-order kinetics, where the number of metal ions outnumbers the number of adsorption sites on clay surface:

$$\ln(q_{eq} - q_t) = \ln(q_{eq}) - k_1 \cdot t \quad (1)$$

where q_{eq} and q_t are the values for the adsorbed amount per unit mass at equilibrium and at any given time t, and k_1 is the pseudo-first-order adsorption rate constant. The k_1 values can be obtained from the angular coefficient of the straight line obtained by plotting the $\ln(q_{eq} - q_t)$ *versus* t graph.

If the validity of the first-order kinetics is weak, the kinetics can be tested for following second-order mechanism as per the rate law expressed by Eq. (2):

$$\frac{t}{q_t} = \frac{1}{k_2 \cdot q_{eq}^2} + \frac{1}{q_{eq}} \cdot t \quad (2)$$

where $k_2 \cdot q_{eq}^2$ is described as the initial adsorption rate when $t \to 0$. The t/qt *versus* t graph provides a straight line allowing obtaining q_{eq} and k_2.

When there is possibility for diffusing the adsorbate species into the adsorbent pores, the intraparticle diffusion rate constant (k_i) can be obtained from Eq. (3):

$$q_t = k_i \cdot t^{0.5} + C \quad (3)$$

In this case, the intraparticle diffusion has a significant effect on the control of the adsorption process kinetics. The q_t *versus* $t^{0.5}$ graph provides a straight line passing by the y axis with an inclination equal to the value of k_i. The values for C provide an approximation of the boundary layer thickness, the greater the C value, the greater the boundary layer effect is. The deviation of the straight line from the origin may be attributed to a difference in mass transfer between the initial and final adsorption stages.

The adsorption equilibrium is usually described by an isotherm equation whose parameters express the surface properties and affinity of the adsorbent, at a pre-set temperature and pH. The isotherms can be adjusted to mathematical models, especially those of Langmuir [13] (Eq. (4)) and Freundlich [14] (Eq. (5)):

$$q_{eq} = \frac{q_m \cdot b \cdot C_{eq}}{1 + b \cdot C_{eq}} \quad (4)$$

where C_{eq} ($mg\,L^{-1}$) and q_{eq} ($mg\,g^{-1}$) are, respectively, the concentration of metal ions in the liquid and solid phases; b and q_m are Langmuir coefficients representing the equilibrium constant for the adsorbate–adsorbent equilibrium and the maximum adsorbed amount on the monolayer.

$$q_{eq} = (K_f \cdot C_{eq})^n \quad (5)$$

where K_f and n are Freundlich coefficients.

The essential characteristics of the Langmuir isotherm can be expressed by a dimensionless number constant, the separation factor or equilibrium parameter (R_L) given by Eq. (6):

$$R_L = \frac{1}{1 + b \cdot C_0} \quad (6)$$

where C_0 ($mg\,L^{-1}$) is the initial concentration of the metal in the liquid phase.

The parameter R_L indicates the curvature of the sorption isotherm: if $R_L > 1$, the isotherm is not favorable; if $R_L = 1$, linear; $0 < R_L < 1$, favorable; $R_L = 0$, irreversible.

The thermodynamic parameters for the adsorption process ΔH (kJ/mol), ΔS (J/(K mol)) and ΔG (kJ/mol) were evaluated using thermodynamic equations (7) and (8):

$$\Delta G = -RT.\ln(K_d) \quad (7)$$

$$\ln(K_d) = -\frac{\Delta G}{RT} = \frac{\Delta S}{R} - \frac{\Delta H}{RT} \quad (8)$$

where K_d is the adsorbate distribution coefficient (=q_{eq}/C_{eq} em L/g); T the temperature (K); R the universal gas constant (8.314×10^{-3} kJ/(K mol)).

The $\ln(K_d)$ *versus* $1/T$ graph must be linear with inclination of the straight line $(-\Delta H/R)$ and intercept the y axis at $(\Delta S/R)$, providing the values for ΔH and ΔS. The variation in Gibbs free energy (ΔG) is the fundamental criterion of process spontaneity.

3. Materials and methods

3.1. Clay adsorbent

In this paper, a Bofe-type bentonite clay from Boa Vista, Paraíba, located in the northeastern region of Brazil, was used as adsorbent. The clay was prepared by size classification, calcined at 500 °C for 24 h in order to increase its mechanical resistance and to eliminate some impurities.

3.2. Clay characterization

The physical–chemical characterization of Bofe clay was performed by energy-dispersive X-ray spectroscopy (EDX) (Oxford, model 7060). This analysis allows the overall chemical composition of a solid to be identified and qualified.

The surface area and volume of pores and micropores were obtained by N_2 physisorption (BET method) at 77 K. These analyses were performed in a Micromeritics Gemini III 2375 Surface Area Analyzer device using the BET method.

The identification of particular clay peaks and maintenance of its properties were obtained by X-ray diffraction (Philips, model X'PERT) (Copper Kα radiation; voltage: 40 kV; current: 40 mA; step size: 0.020 2θ; time per step: 1.000 s; angle of incidence: 3–50°).

The analyses mentioned were carried out for natural and calcined Bofe clay samples before and after nickel adsorption.

3.3. Bath sorption procedure

The adsorption experiments were carried out using an aqueous solution with $Ni(NO_3)_2{\cdot}6H_2O$ at the fixed concentrations in finite bath at controlled temperature under constant stirring at 150 rpm. At specific time intervals, solution aliquots were removed and centrifuged. The supernatant liquid was diluted and its concentration was determined by atomic absorption spectrometry (Perkin Elmer AA Analyst 100 with air-acetylene oxidizing flame).

In this part of the work, the experiments were conducted in five groups to see the effect of adsorbent amount, adsorbate concentration, pH of the adsorbate solution, contact time and temperature. The experimental procedure mentioned above was used in each group by making some minor changes depending on the parameter studied.

During the determination of effect of contact time, the experiments were conducted by using 1 g of clay per 100 mL of solution at 50 mg/L concentration. Temperature and pH were kept as constant at 293 K and 5.3, respectively. The samples were shaken for a time interval between 0 and 250 min.

The effect of pH was studied by changing the pH between 2.0 and 10.0 and by keeping the amount of clay, solution concentration and temperature same as with the kinetics part.

The experiments were repeated with different clay amounts, adsorbate concentration, pH of the adsorbate solution, interaction time and temperature. For maintaining pH of the medium, either 0.01N HNO_3 or 0.01N $NH_4(OH)$ was added in order to set a specific pH value and the pH was monitored both before and after adsorption. The following conditions were maintained for the different sets of experiments:

(i) Kinetics: clay 1 g/100 mL, Ni(II) 50 mg/L, temperature 293 K, pH 5.3, interaction time 250 min. Classical models (Eqs. (1)–(3)) were fitted.

Table 1
Percentage of compounds in Bofe clay.

Element	Molecular (%)		
	Bofe clay *in natura*	Bofe clay calcined	Bofe clay calcined + Ni
Na	0.54	0.50	–
Mg	1.34	1.19	1.12
Al	7.43	6.84	6.75
Si	46. 6	46.17	37.32
K	0.12[a]	–	–
Ca	0.44	0.58	0.29
Ti	0.42	0.53	0.43
Fe	3.58	3.32	3.83
Ni	–	–	0.72
Total	60.85	59.13	49.46

[a] $\leq 2\sigma$.

(ii) Effects of pH: clay 1 g/100 mL, Ni(II) 50 mg/L (0.85 mM), temperature 293 K, interaction time 150 min, pH 2.0–10.0 at unit.
(iii) Effects of adsorbent amount: Ni(II) 50 mg/L, temperature 293 K, pH 5.3, interaction time 150 min, clay 0.5 g, 1 g, 2 g, 3 g and 4 g of clay/100 mL.
(iv) Effects of adsorbate concentration and adsorption isotherm: clay 1 g/100 mL.

Langmuir's theoretical model and Freundlich's empirical model were adjusted to the adsorption isotherms. The adsorbed amount was obtained by Eq. (9):

$$Q = \frac{V(C_i - C_f)}{m} \quad (9)$$

where Q the adsorbed mass of metal ion per gram of adsorbent ($mg\,g^{-1}$); V the volume of solution (L); C_i, C_f the initial and final concentration of metal ion, respectively ($mg\,L^{-1}$); m the mass of adsorbent (g).

(v) Thermodynamics: clay 1 g/100 mL, time 150 min, pH 5.3, temperature 293, 313, 323 and 348 K, Ni(II) concentrations at linear region of isotherm curves where Henry's law for infinite dilution is valid.

4. Results and discussion

4.1. Adsorbent characterization

4.1.1. Chemical composition by EDX

The molecular composition of the compounds *in natura*, calcined and calcined with adsorbed nickel Bofe clays is shown in Table 1. All ions shown in the average composition, except for nickel, have a percentage within the expected for this clay, according to data from Souza Santos [10]. EDX is only a qualitative analysis and was used for understanding the chemical composition of Bofe clay and the corresponding values of percentage of compounds obtained, although an average of three measures should not be quantified. The presence of nickel after adsorption shows that indeed this metal was adsorbed by clay and now appears as part of its chemical composition.

According to the chemical composition analysis, the clay used in this work is a polycationic bentonite due to the presence of Ca^{2+}, Mg^{2+} and Na^{+} cations in natural and calcined clay samples. This type of clay is the most often found one in Brazil [15].

The quantitative C.E.C. values obtained for Bofe clay "*in natura*" and calcined are, respectively, 93.333 ± 5.739 and 55.652 ± 4.260. The smectite clays of Paraíba generally have CEC values between 50 and 90 meq/100 g of clay [10]. The comparatively high CEC value of the "*in natura*" clay indicates that the minerals have a high level of isomorphic substitutions. Moreover the smectite calcined at 500 °C has the ability to exchange cations drastically reduced in relation to the natural clay.

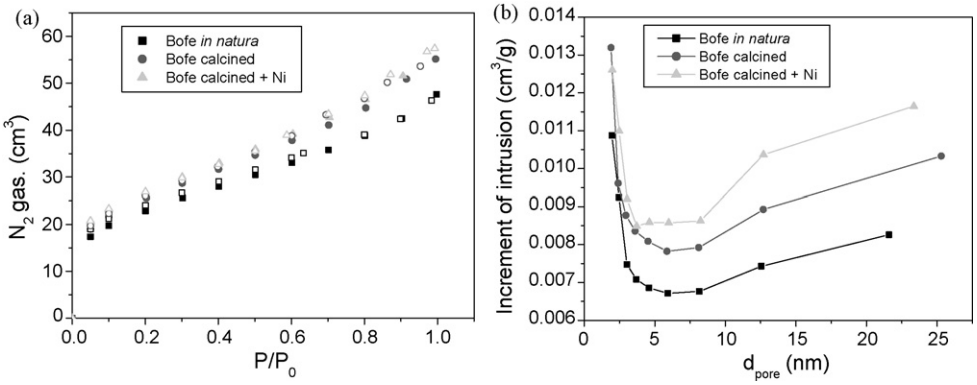

Fig. 1. (a) Adsorption isotherms and N_2 desorption at 77 K. The filled dots represent adsorption and the blank ones, desorption. (b) Increase in intrusion (cm^3/g) *versus* pore diameter (nm) on Bofe clay.

The compound percentages obtained by EDX show that there was virtually no change to the chemical composition of the clay after its calcination, the main elements being preserved, such as silicon and aluminum, as well as to exchangeable cations. With nickel adsorption, there was a reduction in the amount of Ca^{2+} and Mg^{2+} cations and disappearance of Na^+ cations. That indicates that ion exchange occurred in the process, especially with Na+, which is more easily exchangeable because it is monovalent. After nickel adsorption, a small percentage of this ion is found in the clay composition.

Furthermore, from the metal speciation and the pH study performed, the pH of adsorbate solution can be kept below 5.8. Moreover, it has been verified that above pH 5.0 the natural and calcined clays have surface charges very close to neutrality. Thus, with the solid lightly charged (neutral), forces of attraction between the adsorbent and the adsorbate must be of the magnitude of adsorption and/or ion exchange. Therefore, both phenomena (adsorption and ion exchange) probably occur during nickel removal.

4.1.2. N_2 physisorption (BET)

The values obtained for the surface area by the BET method for *in natura*, calcined and calcined with adsorbed nickel Bofe clay samples are found in Table 2. The correspondent N_2 adsorption and desorption isotherms and pore diameter as a function of intrusion increase are shown in Fig. 1. This method was chosen because it presents the best fits of data, when compared to those of the Langmuir model, in addition to the similar behavior of the curves obtained with BET isotherms.

Using BET adsorption isotherms, the volume of micropores (V_{mi}) and mesopores (V_{mes}) is obtained by reading the adsorbed volume (V_{ads}) at P/P_0 = 0.10 and 0.95, expressed by Eqs. (10) and (11) [16]:

$$V_{mi} = V_{ads(P/P_0=0.10)} \quad (10)$$

$$V_{mes} = V_{ads(P/P_0=0.95)} - V_{ads(P/P_0=0.10)} \quad (11)$$

An increase in the surface area (12.8%), as well as in the volume of clay micropores (9.8%) and mesopores (30.1%), is observed after calcination, due to loss by dehydration and dehydroxylation. It is possible that calcination increased the microporosity of the clay and expanded the micropores upon releasing binding water, forming pores in the size range of mesopores.

Table 2
Sample surface area by BET method.

Bofe clay	Surface area (m^2/g)	R^2	V_{mi} (cm^3/g)	V_{mes} (cm^3/g)
In natura	78.8909	0.9996	19.725	24.560
Calcined	89.0191	0.9997	21.660	31.945
Calcined + Ni	92.5897	0.9997	23.356	31.755

With nickel adsorption on the clay, there was a slight increase in the surface area of the clay, with development of microporosity (increase by 7.8%), while the volume of mesopores was slightly reduced (0.6%). The replacement of Na^+ cations with Ni^{2+} cations led to an increase in the lamellar interplanar distance of the clay, which may account for the increase in the surface area of the clay following the nickel adsorption process.

In analyzing the behavior of the isotherms obtained, we can classify them according to Brunauer, Emmet and Teller [17] as type II or BET isotherms, characterized by the formation of adsorbed molecule multilayers on the surface of a solid. This type of sigmoidal (S-shaped) isotherm is often found in solids having pores larger than micropores (mesopores). The Bofe clay presented surface areas that were very favorable for all analyzed samples.

In Fig. 1a, it is observed that the position of the N_2 desorption isotherm virtually coincides with that of adsorption, that is, the hysteresis phenomenon characterizing the irreversibility of the sorption process can be neglected for all analyzed samples. This indicates that nickel adsorption into and desorption from Bofe clay pores is virtually reversible [18].

Fig. 1b shows bands of pore diameter predominant in Bofe clay, which according to the pore diameter classification of IUPAC [18], the pores can be designated as macropores (pores with width larger than 50 nm), mesopores (pores with width between 2 and 50 nm) and micropores (pores with diameter below 2 nm). This figure, together with Table 2, which are presented the volumes of micro and mesopores, indicate the alterations in size of diameter of pores occurring in the clay after calcination and adsorption of nickel. The presence of micropores and mesopores is observed in all Bofe clay samples, with predominance of mesoporosity.

4.1.3. X-ray diffraction

The XRD analysis for clay samples of Bofe *in natura*, before adsorption, calcination and submission to nickel adsorption is shown in Fig. 2. In each diffractogram, for the considered band, there are two characteristic peaks for montmorillonite and the others are related to quartz. To easily identify them, the peaks referring to montmorillonite are marked with letter 'M' and the others related to quartz with letter 'Q'.

Considering the angles that correspond to the montmorillonite peaks and applying Bragg's law ($n\lambda = 2d \sin\theta$), for the λ of 1.542 Å value, d is obtained, which represents the basal interlayer distances of Bofe clay, whose results are shown in Table 3.

It can be observed that the Bofe clay samples analysed are not characterized by a highly crystalline structure, as it is found, for example, in zeolites, since the peaks detected in these samples are well defined. The difficulty in identifying peaks is explained by non-diffraction of X-ray, which had a deviation throughout the process,

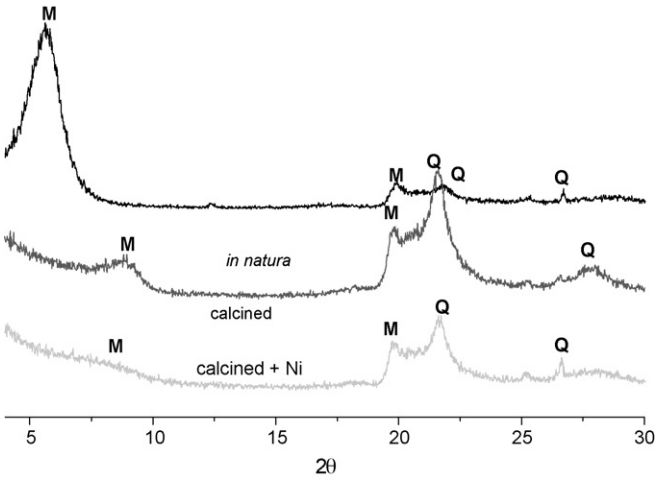

Fig. 2. Diffractogram of Bofe *in natura*, calcined at 500 °C and calcined + Ni adsorbed clays.

what could characterize the formation of an inter-crystalline joint of clays.

Through the diffractograms, there is a significant deviation of the particular montmorillonite peak (Bofe *in natura*) ($2\theta = 5.66°$) for an angle 2θ higher ($8.76° < 2\theta < 8.80°$) obtained for the other samples, which indicates shorter plane interlayer distances (d_{001}).

In Table 3, all samples in the angles of incidence (2θ) between 19.6° and 19.9° regarding the second montmorillonite peak, showed practically the same interlayer basal distances (around 4.5 Å). In the angles of incidence (2θ) between 5.66° and 8.88°, regarding the first montmorillonite peak, the Bofe clay *in natura* sample showed a longer interlayer spacing (d_{001} = 15.6 Å) than that of the calcined clay samples (with or without adsorbed Ni), whose values ranged around 10 Å.

4.2. Nickel speciation and pH_{ZPC}

Fig. 3 shows the speciation curve of the Ni^{2+} ion in aqueous solution with nitrate ions at a concentration of 0.85 mM (50 ppm) determined through the HYDRA application. In the pH range of 6.5–8, the fraction of Ni^{2+} ions in aqueous solution decreases and the formation of nickel hydroxide begins, which is precipitated. To ensure that only the adsorption process will occur, one must use a pH value below that of minimum precipitation, which corresponds to 6.5 for this concentration (50 ppm) and ionic strength.

In addition to the nickel speciation curve obtained by the HYDRA application, another important property to be considered is the pH_{ZPC}, which corresponds to the value at which the surface charges of a suspended solid is zero. The pH_{ZPC} of the natural and calcined Bofe clays (see Fig. 4) was obtained according to the potentiometric titration methodology described by Davranche [19].

Table 3
Identification of montimorillonite peaks and interlayer distance found by Bragg's method.

Bofe clay	Corresponding angle (2θ—grades)	Basal interlayer distance (Å)
In natura	5.66	15.61
	19.8	4.48
Calcined	8.80	10.05
	19.8	4.48
Calcined + Ni	8.76	10.09
	19.6	4.53

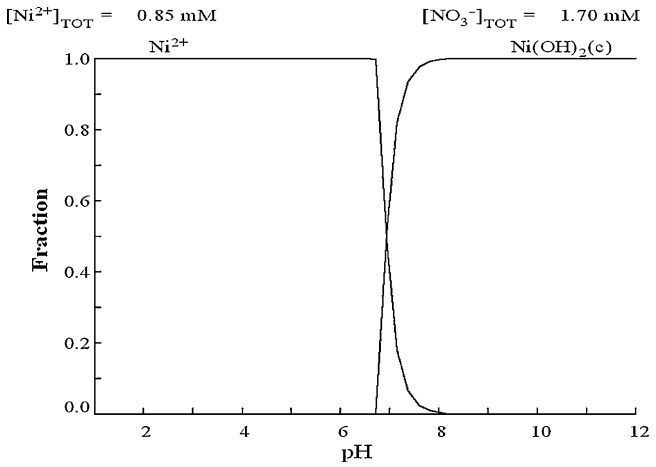

Fig. 3. Ni(II) speciation curve at a concentration of 50 ppm (0.85 mM).

According to Fig. 4, the pH_{ZPC} values obtained for the natural and calcined Bofe clays are, respectively, 6.1 and 5.3. Thus, in order to ensure that the clay surface has a null or negative charge so as to make the adsorption of positively charged metal ions more favorable, the adsorbate solution pH must be kept below 5.3.

The pH of the dispersions formed by the clays Bofe *in natura* and calcined was measured directly, where 1 g of the clay was dispersed in 100 mL of deionized water. The results of this study were 7.78 ± 0.01 and 4.27 ± 0.01 for *in natura* and calcined clay, respectively. The pH of a clay results in part from the nature of exchangeable ions. According to the chemical composition, the exchangeable ions of the *in natura* Bofe clay are cations of alkali metals and alkaline earth metals, which give an alkaline pH to dispersions formed by natural clays. With the calcination, there is no loss of cations, but it occurs the dehydroxylation, which gives an acid pH to the dispersion formed with this state of the Bofe clay.

4.3. Adsorption kinetics

Fig. 5a and b presents the curve for nickel adsorption kinetics at an initial concentration of 41.5 ppm on calcined Bofe bentonite clay at 500 °C (24 h). The adsorption of nickel ions into clay pores is found to occur rapidly at the first moments of the process, remaining virtually at equilibrium over time. The reduction in the concentration of this ion under the condition of this study was 40%, compared to the initial concentration of 50 ppm. The maximum adsorbed amount was 1.91 mg of metal/g of clay.

The adsorption kinetics was adjusted with the pseudo-first-order (Fig. 5c), the second-order kinetics model (Fig. 5d) and

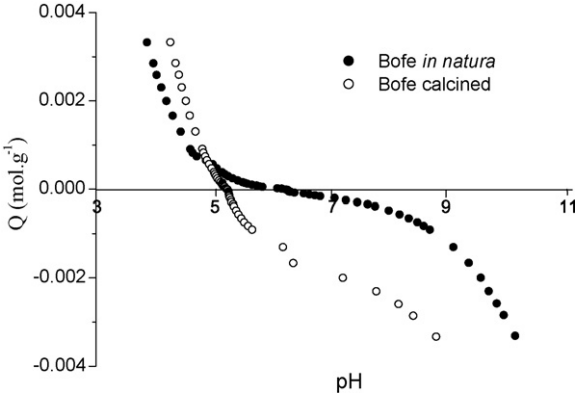

Fig. 4. pH_{ZPC} of Bofe clay *in natura* and calcined.

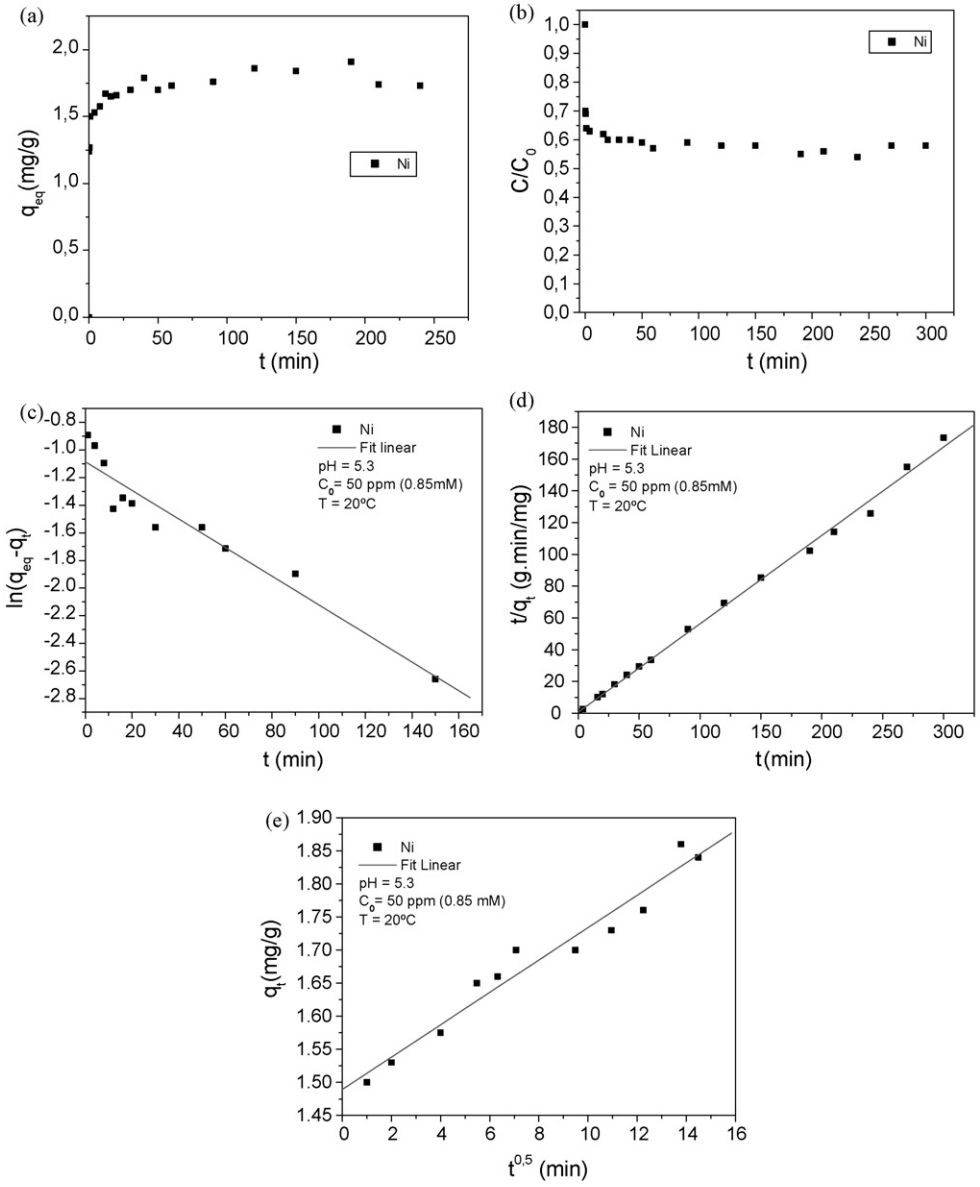

Fig. 5. Kinetic curve for nickel adsorption on calcined Bofe clay. (a) Adsorbed amount at equilibrium; (b) dimensionless solution concentration as a function of adsorption time. Fit of (c) pseudo-first-order kinetic model; (d) second-order kinetic model; (e) intraparticle kinetic model to Ni(II) adsorption on calcined Bofe clay (1 g clay/100 mL solution).

the intraparticle diffusion model (Fig. 5e). The linear correlation coefficients and pseudo-first-order constants (k_1), second-order constants (k_2) and intraparticle diffusion constants (k_i), as well as the equilibrium capacity obtained in Fig. 5 are shown in Table 4.

Actually the existence of two slopes in Fig. 5c indicates two different lines and also second-order mechanism. Moreover the intraparticle diffusion model was less suitable for experimental data if compared with the second-order kinetic model, indicating that the diffusion of metal species into pores is the prevailing factor controlling the process mechanism. The second-order kinetics model showed excellent linearity ($R^2 = 0.99$) and tends to represent more satisfactorily the mechanism of the interactions involved during nickel adsorption into the calcined Bofe clay pores. The values of the experimental q_{eq}, calculated by the second-order model, showed greater agreement, with deviation of 5.7%.

4.4. Effect of pH

According to Peltier and Sparks [20], the influence of pH on the characteristics of Ni(II) ion sorption on clay must be carefully examined and controlled. Fig. 6 and Table 5 show the effect of pH on the process.

Table 4
Ni(II) adsorption rate coefficients for pseudo-first-order and second-order models and intraparticle diffusion on calcined Bofe clay.

Pseudo-first-order (Eq. (1))	Second-order (Eq. (2))	Intraparticle diffusion (Eq. (3))
k_1 = 0.0069 g/(mg min) q_{eq} = 0.35 mg min/g	k_2 = 0.2113 g/(mg min) q_{eq} = 1.80 mg min/g	k_i = 0.0245 mg/(g min) C = 1.4092
R^2 = 0.9009	R^2 = 0.9971	R^2 = 0.9557

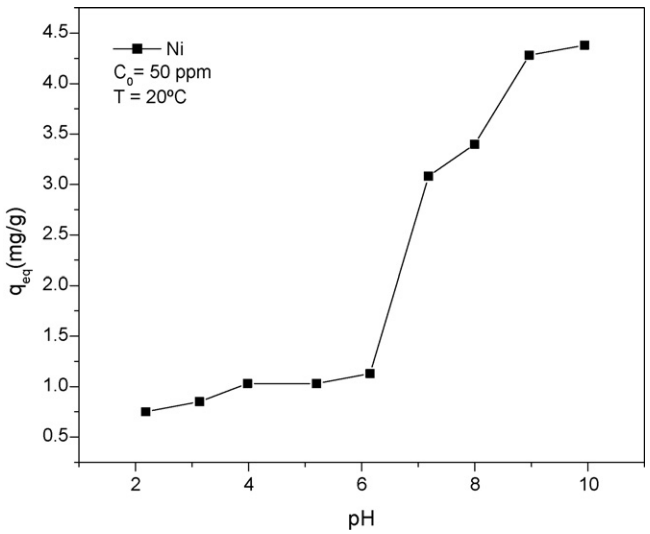

Fig. 6. pH effect on Ni (II) ion removal on calcined Bofe clay.

Table 5
pH effect on Ni(II) ion adsorption and removal percentage on Bofe clay.

pH	C_{eq} (mg/L)	q_{eq} (mg/g)	Rem%
2.18	42.5	0.75	15.00
3.13	41.5	0.85	17.00
3.98	39.75	1.03	20.50
5.2	39.75	1.03	20.50
6.15	38.75	1.13	22.50
7.18	19.25	3.08	61.50
8.00	16.00	3.40	68.00
8.96	7.25	4.28	85.50
9.94	6.25	4.38	87.50

In the pH range analyzed (2–10), there are several forms of Ni(II) ion complexation in aqueous solution. Saline solutions with a number of heavy metals hydrolyze to form several metal hydroxides, which show low solubility in aqueous solution. Therefore, due to the degree of hydrolysis–precipitation, metal cations form hydroxide complexes, depending on the pH range and metal concentration, that is, it is associated with the metal speciation curve at a given concentration.

In Fig. 6, an increase in the removal of metal is seen as the pH of the adsorbate solution increases. In the pH range of 2–6 the adsorption process is predominant. In the range of 6–8, a sharp increase in the amount of removed nickel is observed. According to the speciation of this metal (Fig. 3), the formation of nickel hydroxide starts in this pH range, with the resulting reduction in the Ni^{2+} ion fraction in aqueous solution. For pH values >8.0, a new increase in nickel removal is observed as a result of the chemical precipitation of the metal in the form of hydroxide. Therefore, the Ni(II) adsorption phenomenon in aqueous solution at 50 ppm occurs at pH below 6.0. A similar behavior was obtained by Chen et al. [7] for nickel adsorption on kaolin clay.

Table 6
Effect of the adsorbed amount of Ni(II) at equilibrium on calcined Bofe clay.

$m_{adsorbent}$ (g)	C_{eq} (mg/L)	q_{eq} (mg/g)	Rem%
0.5	29.75	2.35	28.31
1	21.25	2.03	48.80
2	13	1.43	68.67
3	9.75	1.06	76.51
4	7.5	0.85	81.93

Acid activation increases the number of sites responsible for the adsorption of several metal species. In an acidic environment, the concentration of H_3O^+ ions promotes the adsorption of metal ions. Thus, as environment acidity increases, more H_3O^+ ions are increasingly replaced with metal ions on the clay surface.

4.5. Effect of adsorbent amount

Adsorption assays using different clay masses (g)/100 mL of adsorbate solution were carried out in order to assess the effect of adsorbent amount on Ni(II) removal. In Fig. 7a and Table 6, an increase in the removal percentage is noted as the amount of clay used increases. That is expected, because at a fixed initial concentration of sorbate the increase in the adsorbent amount provides a larger surface area or adsorptive sites. However, according to Fig. 7b and Table 6 the adsorbed amount per unit mass of adsorbent (q_{eq}) declines.

The decrease in adsorbed amount per unit mass of adsorbent is a generally observed behavior. It has also reported by the many researchers [21–26]. This may be attributed to two reasons: (i) a large adsorbent amount effectively reduces the unsaturation of the adsorption sites and correspondingly, the number of such sites per unit mass comes down resulting in comparatively less adsorption at higher adsorbent amount, and (ii) higher adsorbent amount creates particle aggregation, resulting in a decrease in the total surface area and an increase in diffusional path length both of which contribute to decrease in amount adsorbed per unit mass [27].

4.6. Adsorption isotherms

The adsorbed amount of metal ions per unit mass of clay (q_{eq}) gradually increases as the initial concentration of the adsorbate solution increases, while the lower the initial concentration is, the

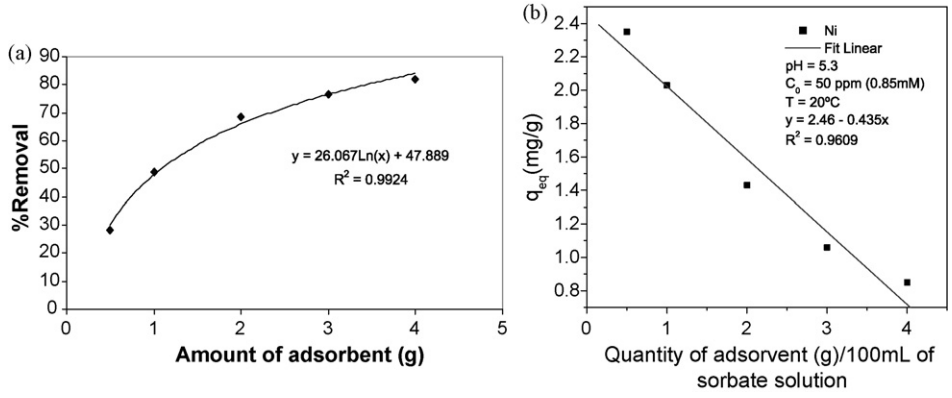

Fig. 7. Effect of the adsorbent amount on adsorption capacity: (a) in Ni(II) removal; (b) at equilibrium.

Table 7
Effect of initial concentration of adsorbate on Ni(II) removal on calcined Bofe clay.

C_0 (mg/L)	C_{eq} (mg/L)	q_{eq} (mg/g)	Rem%
2.66	0.18	0.25	93.23
4.25	0.2	0.40	95.29
14	6	0.80	57.14
16	8	0.80	50.00
27.75	13.5	1.42	51.35
35.5	17.5	1.80	50.70
37	19.5	1.75	47.30
43.75	24.75	1.90	43.43
44.75	24.75	2.00	44.69
61.75	40	2.17	35.22
84.5	59	2.55	30.18
129	105	2.40	18.60
177	153	2.40	13.56

higher the percentage removal becomes, as can be seen in Table 7. With the initial solution at a low concentration, the ratio between the number of ions and the number of adsorptive sites available is small; consequently, adsorption depends on the initial concentration. Therefore, as the concentration of ions increases, adsorption increases as well. At high ion concentrations, each unit mass of adsorbent is subjected to a larger number of ions, which gradually fill up the sites. Thus, an increase in q_{eq} and a reduction in the adsorbed percentage are observed.

Adsorption isotherms were obtained, which associate equilibrium concentrations in the solid and liquid phases at a given process temperature. Thermodynamic data were obtained through the static method in thermostatic finite bath under constant stirring for four different temperatures (20, 40, 50 and 75 °C) and correlated by the Langmuir and Freundlich isotherms. Fig. 8 shows the adsorption isotherms for 1 g clay/100 mL adsorbate solution, adjusted by the Langmuir and Freundlich models, at initial nickel concentrations ranging from 3 to 200 ppm.

The parameters of these models, expressed by Eqs. (4) and (5), were associated with the process temperature. The Langmuir and Freundlich models were adjusted to experimental data through the Gauss–Newton nonlinear estimation method in the Statistic 7.0 for Windows® software. The regression coefficients for both adjustments are shown in Table 8.

Using the adsorption isotherms, the maximum adsorbed capacity is observed to increase as the process temperature rises, which means that an increase in energy favors the adsorption on the clay surface. This behavior indicates an enthalpy variation during positive adsorption or endothermic process. However, this behavior is inverted in Henry's infinite dilution region, that is, at very low concentrations (up to 10 ppm).

It is also seen in Fig. 8 and Table 8 that the Langmuir model was the one that best represented the experimental adsorption

Table 8
Langmuir parameters (1 g Bofe clay/100 mL Ni(II) solution).

T (°C)	Langmuir			Freundlich		
	q_m	b	R^2	K_f	n	R^2
20	2.8752	0.07095	0.9693	0.2115	0.30230	0.9282
40	3.0719	0.09095	0.9788	0.3095	0.29910	0.9492
50	3.0470	0.12409	0.9628	0.3153	0.30256	0.9406
75	3.8930	0.05557	0.9825	0.3807	0.32749	0.9663

Table 9
Separation factor values (R_L) for Ni(II) adsorption by Bofe clay.

C_0 (mg/L)	20 °C	40 °C	50 °C	75 °C
2.66	0.8412	0.8052	0.7518	0.8712
4.25	0.7683	0.7212	0.6547	0.8089
9.5	0.5974	0.6026	0.4590	0.6545
14	0.5017	0.5365	0.3653	0.5624
16	0.4683	0.4399	0.3350	0.5293
19	0.4259	0.3666	0.2978	0.4864
27.5	0.3388	0.2856	0.2266	0.3955
35.5	0.2842	0.2365	0.1850	0.3364
43.75	0.2437	0.1972	0.1555	0.2914
61.75	0.1858	0.1511	0.1154	0.2257
85	0.1422	0.1145	0.0866	0.1747
130	0.0978	0.0780	0.0584	0.1216
177	0.0737	0.0585	0.0435	0.0923

isotherm data for the four different process temperatures. The Langmuir isotherm is specific for monolayer adsorption, which was the case in this work, while the Freundlich model is better applied to adsorption at heterogeneous sites on the surface of a solid, with a mechanism that has not been established yet. The Langmuir equilibrium coefficient b determines the direction to which the equilibrium adsorbate–adsorbent clay (solid phase) + Ni(II) (aqueous phase) = clay – Ni(II) moves. Higher values indicate that the equilibrium moves to the right side, with the resulting formation of the adsorbate–adsorbent complex.

The values obtained for the Freundlich constant (n) are around 0.3. According to Treybal [28], this range indicates that the adsorptive characteristics of the clay are good for nickel sorption.

The values calculated for R_L (Eq. (6)), determined by using the Langmuir constant obtained by the nonlinear method *versus* the initial nickel concentration for four temperatures is in Table 9. According to the separation values, it is observed that under the four process temperature conditions nickel sorption is considered favorable ($0 < R_L < 1$), being more favorable for higher initial concentrations of metals.

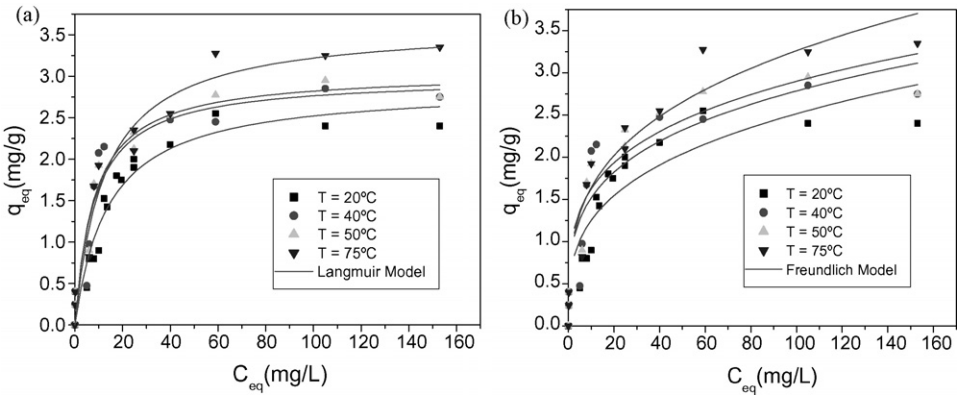

Fig. 8. Adsorption isotherms for calcined Bofe clay (1 g clay/100 mL solution, pH 5.3) adjusted to the models of: (a) Langmuir; (b) Freundlich.

Table 10
Thermodynamic parameters of adsorption (1 g Bofe clay/100 mL Ni(II) solution).

T (°C)	T (K)	K_d (L/g)	ΔG (J/mol)	ΔH (kJ/mol)	ΔS (J/(K mol))
20	293.15	1.7690	−1390.24	−7.33	−20.33
40	313.15	1.4568	−979.56		
50	323.15	1.2889	−681.85		
75	348.15	1.1069	−293.98		

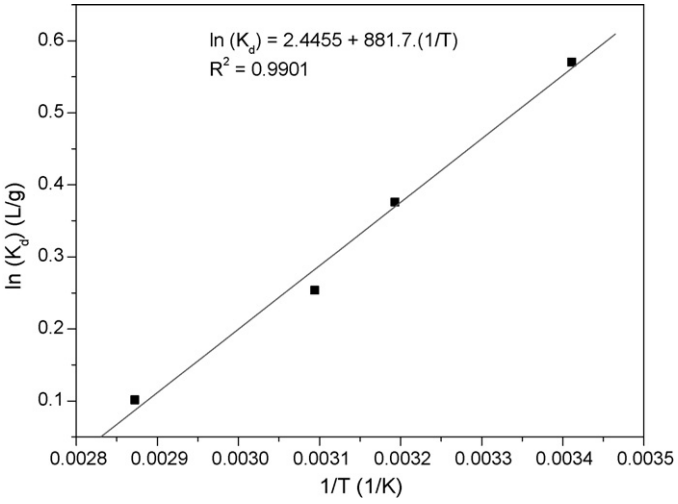

Fig. 9. Langmuir parameters as a function of temperature.

4.7. Adsorption thermodynamics

The thermodynamic parameters ΔH, ΔS and ΔG (Eqs. (7) and (8)) presented in Table 10 were obtained from Fig. 9. The negative ΔH indicates that the process is exothermal, confirming the adsorption theory. The magnitude of the enthalpy variation achieved (−7.33 kJ/mol) is in the range of physisorption processes, with weak van der Waals bonds between the ions and the mineral clay. A decrease in entropy during adsorption helps the stabilization of the complex formed between the metal and the clay ($\Delta S < 0$).

The clay–Ni interactions occurred spontaneously and were not accompanied by a decrease in Gibbs free energy ($\Delta G < 0$). Negative ΔS values suggest a decrease in randomness at the solid/solution interface during nickel sorption on Bofe clay. However, the degree of spontaneity was found to decline as the process temperature rose, ranging from −1.39 to −0.29 kJ/mol for the temperature range between 20 and 75 °C.

5. Conclusions

The analysis of the chemical composition of the Bofe clay by EDX indicated that it has a molecular percentage of compounds within the expected for this type of clay and can be classified as polycationic. The reduction in the amount of exchangeable cations after nickel adsorption indicated that ion exchange took place in the process, especially with Na^+, which is more easily exchangeable since it is monovalent. Therefore, both phenomena (adsorption and ion exchange) probably occur during nickel removal.

N_2 physisorption isotherms obtained can be classified as type II or BET, characterized by the formation of adsorbed molecule multilayers on the surface of a solid, typical of non-porous solids or solids having pores larger than micropores. Calcination causes an increase in the surface area and development of micro and mesoporosity in the clay due to the release of binding water and dehydroxylation. With nickel adsorption on the clay, there was a slight increase in the surface area of the clay, with development of microporosity and slight reduction in mesoporosity.

The obtained diffractograms show that the analysed Bofe clay samples are not characterized by a highly crystalline structure. All samples, in the angles of incidence between 9.80° and 9.95°, corresponding to the montimorillonite second peak, showed the same basal distance (4.5 Å). In angles of incidence between 2.83° and 4.44°, corresponding to the first montimorillonite peak, the sample of Bofe clay *in natura* showed a basal distance (15.6 Å) greater than the ones obtained from calcined samples (with or without adsorbed nickel) with a value range around 10 Å.

According to the nickel speciation curve and to the pH_{ZPC} obtained for the calcined Bofe clay, the pH of the adsorbate solution must be kept below 5.3 so as to ensure that the clay surface will be more favorable for the adsorption of positively charged metal ions and that chemical precipitation will not occur.

The second-order kinetic model was the one that best represented the mechanism of interactions involved during nickel adsorption into the pores of the calcined Bofe clay.

There was an increase in removal percentage and the adsorbed amount per unit mass of adsorbent (q_{eq}) decreased as the amount of clay used increased. The adsorbed amount of metal ions per unit mass of clay (q_{eq}) gradually increases with the increase in the initial concentration of the adsorbate solution, while the removal percentage increases as the initial concentration decreases.

The adsorption isotherms were better represented by the Langmuir model for the four different process temperatures. The thermodynamic study showed that the nickel adsorption process on Bofe clay is exothermal, with the magnitude of enthalpy variation in the range of physisorption processes, and clay–Ni interactions occurred spontaneously, being followed by a decrease in Gibbs free energy ($\Delta G < 0$). However, the degree of spontaneity was found to decline as the process temperature rose.

Acknowledgements

The authors acknowledge the financial support received from CNPq, CAPES and Foundation for Research Support of São Paulo State, FAPESP, for this research.

References

[1] R.C.S.S. Seet, A. Johan, C.E.S. Teo, S.L. Gan, K.H.L. Chest, Inhalational nickel carbonyl poisoning in waste processing workers, ProQuest Medical Library (2005) 424.
[2] V.R. Ouhadi, R.N. Yong, M. Sedighi, Desorption response and degradation of buffering capability of bentonite, subjected to heavy metal contaminants, Eng. Geol. 85 (1–2) (2006) 102–110.
[3] T. Novakovic, L. Rozic, S. Petrovic, A. Rosic, Synthesis and characterization of acid-activated Serbian smectite clays obtained by statistically designed experiments, Chem. Eng. J. 137 (2) (2008) 436–442.
[4] P. Stathi, K. Litina, D. Gournis, T.S. Giannopoulos, Y. Deligiannakis, Physicochemical study of novel organoclays as heavy metal ion adsorbents for environmental remediation, J. Colloid Interface Sci. 316 (2) (2007) 298–309.
[5] K.G. Bhattacharyya, S.S. Gupta, Adsorption of a few heavy metals on natural and modified kaolinite and montmorillonite: a review, Adv. Colloid Interface 140 (2) (2008) 114–131.
[6] S.M.I. Sajidu, I. Persson, W.R.L. Masamba, E.M.T. Henry, Mechanisms of heavy metal sorption on alkaline clays from Tundulu in Malawi as determined by EXAFS, J. Hazard. Mater. 158 (2–3) (2008) 401–409.
[7] W.J. Chen, L.C. Hsiao, K.K.Y. Chen, Metal desorption from copper(II)/nickel(II)-spiked kaolin as a soil component using plant-derived saponin biosurfactant, Process Biochem. 43 (5) (2008) 488–498.
[8] O. Abollino, M. Aceto, M. Malandrino, C. Sarzanini, E. Mentasti, Adsorption of heavy metals on Na-montmorillonite. Effect of pH and organic substances, Water Res. 37 (7) (2003) 1619–1627.
[9] E.F. Covelo, F.A. Vega, M.L. Andrade, Sorption and desorption of Cd, Cr, Cu, Ni, Pb and Zn by a Fibric Histosol and its organo-mineral fraction, J. Hazard. Mater. 159 (2–3) (2008) 342–347.
[10] P. Souza Santos, Science and Technology of Clays, vols. 1–3, 2nd ed., Edgard Blücher Ltd., São Paulo, 1992 (in Portuguese).

[11] J.L. Lummus, J.J. Azar, Drilling Fluids Optimization: A Practical Field Approach, Oklahoma, PennWell Publishing Company, Tulsa, 1986.
[12] S. Lagergren, Zur theorie der sogenannten adsorption gelöster stoffe. Kungliga Svenska Vetenskapsakademiens Handlingar, 24(4) (1898) 1-39.
[13] I. Langmuir, The adsorption of gases on plane surfaces of glass, mica and platinum, J. Am. Chem. Soc. 40 (1918) 1361–1403.
[14] H.M.F. Freundlich, Über die adsorption in lösungen, Zeitschrift fur Physikalische Chemie (Leipzig) 57A (1906) 385–470.
[15] L.V. Amorim, J.D. Viana, K.V. Farias, M.I.R. Barbosa, H.C. Ferreira, Revista Matéria 11 (1) (2006) 30–40 (in Portuguese).
[16] J.G. Gomez, A.M. Garcia, M.A.D. Diez, C.G. Garcia, E.S. Rey, Preparation and characterization of activated carbons from impregnation pitch by $ZnCl_2$, Appl. Surf. Sci. 252 (2006) 5976–5979.
[17] S. Brunauer, P.H. Emmet, E. Teller, Adsorption of gases in multimolecular layers, J. Am. Chem. Soc. 60 (1938) 309–319.
[18] IUPAC, Physical Chemistry Division. Commission on Colloid and Surface Chemistry including Catalysis, Reporting physisorption data for Gas/Solid Systems with Special Reference to the determination of Surface Area and Porosity, Pure Appl. Chem. 57 (4) (1985) 603–619.
[19] M. Davranche, S. Lacour, F. Bordas, J.C. Bollinger, An easy determination of the surface chemical properties of simple and natural solids, J. Chem. Educ. 80 (1) (2003) 76–78.
[20] E. Peltier, D.L. Sparks, The influence of surface precipitation on nickel solubility, bioavailability and fate in contaminated soils, in: Proceedings of the 18th World Congress of Soil Science, Philadelphia, 9–15 July, 2006.
[21] S.S. Gupta, K.G. Bhattacharyya, Immobilization of Pb(II), Cd(II) and Ni(II) ions on kaolinite and montmorillonite surfaces from aqueous medium, J. Environ. Manage. 87 (1) (2008) 46–58.
[22] K. Al-Malah, M.O.J. Azzzam, N. Abu-Lail, Olive mills effluent (OME) wastewater post-treatment using activated clay, Sep. Purif. Technol. 20 (2000) 225–234.
[23] Y.-H. Shen, Removal of phenol from water by adsorption flocculation using organobentonite, Water Res. 36 (2002) 1107–1114.
[24] S. Al-Asheh, F. Banat, L. Abu-Aitah, Adsorption of phenol using different types of activated bentonites, Sep. Purif. Technol. 33 (2003) 1–10.
[25] S. Yapar, V. Özbudak, A. Dias, A. Lopes, Effect of adsorbent concentration to the adsorption of phenol on hexadecyl trimethyl ammonium-bentonite, J. Hazard. Mater. B121 (2005) 135–139.
[26] B. Yu, Y. Zhang, A. Shukla, K.L. Dorris, The removal of heavy metal from aqueous solutions by sawdust adsorption—removal of copper, J. Hazard. Mater. B 80 (2000) 33–42.
[27] A. Shukla, Y.-H. Zhang, P. Dubey, J.L. Margrave, S.S. Shukla, The role of sawdust in the removal of unwanted materials from water, J. Hazard. Mater. 95 (2002) 137–152.
[28] R.E. Treybal, Mass Transfer Operations, 3rd ed., McGraw Hill, New York, 1980.